Relationship between pharyngeal airway depth and ventilation condition in mandibular setback surgery: A computational fluid dynamics study

Journal:	*Orthodontics and Craniofacial Research*
Manuscript ID	OCR-2019-12-322-ORI.R1
Manuscript Type:	Original Article
Research Area:	Surgery, Craniofacial anomalies, Human study, Imaging
Keywords (Please write 3 to 5 keywords according to Index Medicus):	skeletal Class III, mandibular setback surgery, pharyngeal airway depth, obstructive sleep apnea, computational fluid dynamics

ABSTRACT

Objectives: This study aimed to determine the anteroposterior depth (APD) of the pharyngeal airway (PA) where postoperative PA obstruction was predicted, using computer fluid dynamics (CFD), in order to prevent obstructive sleep apnea after mandibular setback surgery.

Settings and sample population: Nineteen skeletal Class III patients (8 men; mean age, 26.7 years) who required mandibular setback surgery had computed tomography images taken before and 6 months after surgery.

Methods: The APD of each site of the four cross-sectional reference planes (retropalatal airway [RA]), second cervical vertebral airway, oropharyngeal airway, and third cervical vertebral airway) were measured. The Maximum negative pressure (Pmax) of the PA was measured at inspiration using CFD, based on a three-dimensional PA model. Inter-site differences were determined using analysis of variance and the Friedman test with Bonferroni correction. The relationship between APD and Pmax was evaluated by Spearman correlation coefficients and non-linear regression analysis.

Results: The smallest PA site was the RA. Pmax was significantly correlated with the APD of the RA ($r_s = 0.628$, $P < 0.001$). The relationship between Pmax and the APD-

RA was fitted to a curve, which showed an inversely proportional relationship of Pmax to the square of the APD-RA. Pmax substantially increased even with a slight reduction of the APD-RA. In particular, when the APD-RA was 7 mm or less, Pmax increased greatly, suggesting that PA obstruction was more likely to occur.

Conclusions: The results of this study suggest that APD-RA is a useful predictor of good PA ventilation after surgery.

(Word; 249/250)

Key words: skeletal Class III, mandibular setback surgery, pharyngeal airway depth, obstructive sleep apnea, computational fluid dynamics

INTRODUCTION

Riley et al. [1] reported concerns about the onset of obstructive sleep apnea (OSA) after narrowing of the pharyngeal airway (PA) due to mandibular setback surgery. To investigate the ventilation condition of the PA after mandibular setback surgery, many studies [2-12] have evaluated PA morphological parameters, such as the anteroposterior depth (APD), lateral width (LAW), cross-sectional area (CSA), and the volume of the PA, using cephalograms and computed tomography (CT). However, it is not clear how reliable these morphological measurements accurately reflect the ventilation condition of the PA.

Computer fluid dynamics (CFD) analysis reproduces the air flow and effectively represents the airway ventilation condition. [13-17] CFD is very effective for the evaluation of upper-airway ventilation conditions, as it can evaluate the flow of air in a manner similar to that during actual breathing, even in cases with complicated upper airways. [18] A few studies [16,17] have evaluated the PA ventilation condition after mandibular setback surgery using CFD. Shar et al. [16] reported that the pressure reduction is enhanced because the PA volume is decreased with mandibular retraction. Yajima et al. [17] reported that the pressure reduction becomes marked when the CSA of the retropalatal airway (RA) is 100 mm^2 or less. However, the ventilation condition has not yet been evaluated using CFD based on the APD of the PA, which was similar to the cephalometric APD of the PA, in a three-dimensional (3D) model. If this were possible, it would enable prediction of the ventilation condition of the PA by cephalometric APD of the PA after mandibular setback surgery. This would also be an effective diagnostic method for preventing obstruction by guiding decisions regarding mandibular position during orthodontic mandibular setback surgery.

Therefore, this study investigated whether the ventilation condition of the PA, as assessed via PA pressure (outcome variable), after mandibular setback surgery could be predicted based on the APD of the PA (predictor variable), as determined by cephalometry and CFD.

Materials and Methods

PATIENTS

This prospective study included 24 patients (14 women, 10 men) who underwent bilateral sagittal split ramus osteotomy of the mandible (without other procedures, such as maxillary osteotomies) for the correction of skeletal

Class III (ANB < 0 degrees) malocclusion. Mandibular setback surgery (amount of mandibular setback, mean and SD = 5.77 ± 2.09 mm, range = 3.83 mm to 10.5 mm) was performed for all patients at the Kanazawa University, Department of Oral and Maxillofacial Surgery, during the period from March 2016 to November 2018. As head posture (all assessments were performed with the patient in a supine position) is known to influence PA volume, an additional inclusion criterion was a craniocervical inclination angle of 90 to 100 degrees. [19] The exclusion criteria comprised patients with craniofacial anomalies, cleft lip and palate, BMI > 30, previous maxillofacial surgery, and symptoms of obstructive sleep apnea such as Epworth Sleepiness Scale (ESS). All operations were performed by the same oral and maxillofacial surgeon (K.O.). Preoperative CT scans (Light Speed Plus; GE Healthcare, Milwaukee, WI, USA) were performed before mandibular setback surgery. All patients were scanned in the supine position, with instructions to hold their breath at the end of expiration, and to refrain from swallowing. Postoperative CT scans were performed at approximately 6 months (5.8 ± 0.7 months) after mandibular setback surgery to confirm proper osteotomy, fixation, and jaw position. After exclusion criteria were applied, 19 patients were included (11 women, 8 men, mean age 26.7 ± 8.4 years, SNA = 80.74 ± 2.86 degrees, SNB = 82.18 ± 2.69 degrees, body mass index = 22.1 ±

3.8 kg/m^2). The serial CT images of these patients were analyzed randomly, without identifying information, to eliminate bias and maintain anonymity. ESS was used to assess symptoms associated with sleep-disordered breathing, such as daytime sleepiness before and after setback surgery. This study was conducted in accordance with the Code of Ethics of the World Medical Association (Declaration of Helsinki), and was approved by the institutional review boards of Kagoshima University, Japan, (180073 (657) Epi-ver. 1) and Kanazawa University (Ethics Committee No. 1594). Informed consent was obtained from all participating patients.

MORPHOLOGICAL ANALYSIS

Cephalometric images were reconstructed from the CT data as described previously. [20] Definitions of landmarks, reference planes, and cephalometric angular measurements were taken from these reconstructed cephalometric images (Fig. 1A). Traditional measurements [10,21] were used to determine the positions of the maxilla and the mandible. The horizontal (x) and vertical (y) positions of the selected landmarks were described based on coordinates relative to a reference plane parallel to the Frankfort horizontal plane, and passing through the sella, with the sella as the origin. To evaluate the PA, 3D images were reconstructed from the CT data as described previously (Fig. 1B and

1C).[20] The following cross-sectional planes were used to segment the airway into regions: (1) the palatal plane, a plane parallel to the hard palate passing through the posterior nasal spine; (2) the retropalatal airway plane (RA plane), a plane parallel to the palatal plane passing through the narrowest point on the soft palate; (3) the second cervical vertebra airway plane (CV_2 plane), a plane parallel to the palatal plane passing through the base of the second cervical vertebra; (4) the oropharyngeal plane (OA plane), a plane parallel to the palatal plane, passing through the midpoint of gonion bilaterally; and (5) the third cervical vertebral airway plane (CV_3 plane), a plane parallel to the palatal plane passing through the most inferior anterior point of the third cervical vertebra (Fig. 1B and 1C). The RA cross-sectional airway was measured parallel to the palatal plane at the narrowest part of the airway on the cephalometric image. The CV_2A cross-sectional airway was measured along the CV_2 plane. The OA cross-sectional airway was measured along the OA plane. The CV_3A cross-sectional airway was measured along the CV_3 plane. In this study, PA cross-sectional measurements included the APD, LAW, and CSA.

EVALUATION OF PA VENTILATION CONDITION

A 3D reconstruction of the PA was generated from the CT data using volume-rendering software (Intage Volume Editor; Cybernet, Tokyo, Japan). Subsequently, using mesh-morphing software (DEP Mesh Works/Morpher; IDAJ Co, Ltd, Kobe, Japan), the 3D model was converted to a smoothed model, without losing the patient-specific shape of the airway.

CFD was used to evaluate the ventilation of the PA models (Fig. 1D–1F). The models were exported to fluid dynamics software (Phoenics; CHAM-Japan, Tokyo, Japan) in stereolithographic format, and the fluid was assumed to be Newtonian, homogeneous, and incompressible. Elliptic-staggered equations and the continuity equation were used in the analysis. [22] The CFD of the PA models was analyzed under the following conditions: air flowing in the nares at a volumetric flow rate of 500 cm^3/s, no-slip condition at the wall surface, mesh-independent, a mesh size of 0.42 mm, and 300 iterations to calculate mean values. The flow pattern was based on the turbulent KECHEN model. Convergence was judged by monitoring the magnitude of the absolute residual sources of mass and momentum, normalized to the respective inlet fluxes. Iteration was continued until all residuals were below 0.2%. The simulation estimated the airflow pressure and velocity of the RA, CV_2A, OA, and CV_3A.

STATISTICAL ANALYSES

Paired t-tests were used to compare PA morphological parameters before and after mandibular setback surgery. The Wilcoxon signed-rank test was used to compare ventilation conditions before and after mandibular setback surgery. Inter-airway site differences of PA morphological parameters were determined using repeated-measures analysis of variance with Bonferroni correction. Inter-airway site differences of ventilation conditions were determined using the Friedman test with Bonferroni correction. Spearman correlation coefficients were calculated to evaluate relationships between morphological measurements and ventilation conditions of both preoperative and postoperative data. For all tests, $P < 0.05$ was considered statistically significant. To calculate the β error, a power analysis was performed ($1 - \beta$ error = 0.80, $\alpha = 0.05$, two-tailed test). The results confirmed the adequacy of the sample size.

For intra- and inter-examiner reliability, a random number generator was used to select 10 patients. Measurements were repeated 1 week after the initial measurements. Both intra- and inter-examiner reliability tests exhibited high correlation ranging from 0.978 to 0.987 for all measures.

Results

MORPHOLOGICAL ANALYSIS

The mandible was significantly displaced backward and upward after mandibular setback surgery (Table 1). The hyoid bone was significantly moved backward and downward after mandibular setback surgery. However, the maxilla was not significantly changed. There was no significant difference in the ESS score before and after surgery (Table 1).

Both before and after mandibular setback surgery, the APD, LAW, and CSA of the RA were significantly smaller than those of any other site (Table 2). APD and CSA were smallest at the RA in all patients. The APD of the RA was significantly decreased after mandibular setback surgery (8.87 ± 2.38 mm), by approximately 30% relative to before mandibular setback surgery (12.61 ± 2.53 mm). Additionally, the APD of the CV_2A, OA, and CV_3A was significantly decreased, similarly to the RA (Table 2).

The LAW of the RA, CV_2A, and OA was significantly decreased after mandibular setback surgery, by approximately 15%. Consequently, the CSA of the

CV_2A, OA, and CV_3A was significantly decreased after mandibular setback surgery, by approximately 30% (Table 2).

CFD

The velocity of the airflow was significantly faster in the RA than at any other site, both before and after mandibular setback surgery (Table 2). The velocity of the airflow in the RA significantly increased by approximately 180% after mandibular setback surgery (Table 2). Additionally, the treatment change ratio (postoperative value/ preoperative value) was larger at this site than at any other site.

The negative pressure was larger at the CV_3A than at any other site, both before and after mandibular setback surgery. The negative pressure of the RA was significantly increased, by approximately 400%, after mandibular setback surgery (Table 3). The velocity and pressure at the other sites (CV_2A, OA, and CV_3A) showed similar changes. Therefore, there were no significant differences in the treatment change ratios of pressure among these sites (Table 2).

CORRELATION ANALYSIS

Maximum negative pressure (Pmax) was positively correlated with the APD and CSA at all sites (Table 3). In particular, the APD of the RA and CSA of the RA were most strongly correlated with Pmax, compared to those parameters for any other site (CV_2A, OA, and CV_3A) (Table 3). Maximum velocity showed similar negative relationships with the APD and CSA of the RA (Table 3). However, there was no significant correlation between the amount of mandibular setback and the change of airway ventilation condition (Bx change vs. Vmax change, rs = 0.093, P = 0.705; Bx change vs. Pmax change, rs = -0.095, P = 0.700, respectively).

REGRESSION ANALYSIS

The distributions of the CSA of the RA and Pmax of the cases in this study are shown in Figure 2A. The relationship between Pmax and the CSA of the RA was represented by a fitted curve that was inversely proportional to the square of the CSA of the RA between preoperative and postoperative data (Fig. 2A). When the CSA of the RA became 100 mm^2 or less, the Pmax was markedly increased (Fig. 2A).

The distributions of the APD of the RA and the Pmax of the cases in this study are shown in Figure 2B. However, one case was an outlier (before and after; although the APD of the RA was small, the Pmax was relatively low) (Fig. 2B; red arrows). The relationship between Pmax and the APD of the RA was represented by a fitted curve (Fig.2B). When the APD of the RA became 7 mm or less (Fig. 2B), the Pmax greatly increased.

Figure 3 shows changes in the pressure of the PA before and after mandibular setback surgery with a similar degree of mandibular retraction. Figure 3A shows sufficient preoperative APD-RA; in this case, there was no major change in the ventilation state of the PA after surgery. Figure 3B shows a small preoperative APD-RA; in this case, the negative pressure greatly increased after surgery. When APD-RA became 7 mm or less, regardless of an equivalent degree of mandibular retraction, the negative pressure increased.

Discussion

This study evaluated changes in the ventilation condition of the PA after mandibular setback surgery, by using both conventional morphological evaluation and CFD evaluation. Consequently, when the APD of the RA was small (7 mm or less), the increase in the negative pressure of the PA was considerable and obstruction of the PA could easily occur.

EVALUATION OF THE PA SITE

The cross-section of the PA varies greatly from the nasopharyngeal to the hypopharyngeal airway. The site of the smallest PA cross-section is thought to influence ventilation conditions, [23] and evaluation of this site is therefore important. However, in previous studies, [2-5,7,12,17,24-27] the evaluation sites differed due to head posture (craniocervical inclination), tongue posture, and scan position. [19,28]

Representative evaluation sites were used in the present study, in order to determine the site that influences the PA ventilation condition the most. Both before and after mandibular setback surgery, the APD, LAW, and CSA at the RA were the smallest of all the sites (CV2A, OA, and CV3A), and the velocity of airflow in the RA was most rapid among all sites, according to CFD. Numerous reports [2,3,12,24] have shown that the RA is the smallest site in the PA. In another CFD study, Dowing and Ku [23] reported that velocity of airflow was fastest in the narrowest part in a CFD model. Other previous CFD studies reported that air flow velocity was most rapid at the RA, among all sites of the PA. [18,29] We conclude that the RA is the most influential site for ventilation conditions at the PA.

POSTOPERATIVE PA CHANGES

With a mandibular retraction of 6–8 mm, the APD of the PA is reduced by around 2–4 mm. [2,3] The results of the present study showed that the APD of the RA was reduced from 12.61 mm (before surgery) to 8.87 mm (after surgery), similar to previous reports. [2,3] Moreover, the LAW of the PA showed a similar tendency. Tebeck et al.[4] investigated the CSA of the RA before and after mandibular setback surgery for patients with Class III, using CT images. The mean CSA of the RA decreased from 181 mm^2 to 158 mm^2. The results of the present study were consistent with these previous findings. [2,4] Our results showed that mandibular setback surgery caused approximately 30%, 15%, and 30% reductions in the APD, LAW, and CSA, respectively. We also found tendencies for similar ratios of reduction in the other sites (CV_2A, OA, and CV_3A). Thus, mandibular setback surgery similarly influenced PA shape at tongue base sites (CV_2A, OA, and CV_3A) and at the soft palate site of the PA.

CFD ANALYSIS

In our study, before mandibular setback surgery, the mean Pmax was -16.05 Pa and the mean maximum airflow velocity was 3.23 m/s; these are similar to the previously reported Pmax (-20 Pa) and velocity (3–4 m/s) in adults without obstruction.[29,30] However, after mandibular setback surgery, the mean Pmax decreased to -40.63 Pa, and the mean maximum velocity increased to 5.81 m/s. Using polysomnography and CFD, Zhao et al. [14] evaluated the effect of mandibular advancement splints (MAS) in a model of the PA for adult OSA. This model did not include the nasal airway. They reported that when negative pressure was greater than -50 Pa, OSA symptoms were detected. Based on these reports [14,29,31] and our results, we suggest that obstruction might occur if the negative pressure of the PA is greater than -50 Pa. A large negative pressure in the PA on inspiration, coupled with muscle relaxation, may present with a higher risk of PA collapse during sleep.

The rate of change in ventilation (i.e., velocity and pressure) of 180–400% caused by mandibular setback surgery was markedly greater than the rate of change in morphology (15–30%). This is potentially because postoperative average pressure and velocity became very large due to the markedly negative pressure that was produced in cases with a CSA of the RA of 100 mm^2 or less (APD of 7 mm or less) (Fig. 2B and 3).

In our study, there was no significant correlation between the amount of mandibular setback and the CFD value. This may be due to the fact that the CFD value is inversely proportional to APD-RA. Therefore, both the amount of mandibular setback and the APD-RA before surgery are needed to determine the CFD value.

PA FORM AND CFD

Only a few studies have investigated the association of CFD findings with the PA form before and after mandibular setback surgery. [16,17] Yajima et al. [17] reported that the decrease in pressure is inversely proportional to the square of the CSA, based on the Hagen–Poiseuille law. [27] In previous studies, [12,24] the CSA in patients with OSA was reported to be 40–79 mm^2. In this study, the maximum negative pressure was -35.7 Pa when the CSA of the RA was 120 mm^2, and -45.7 Pa when the CSA was 100 mm^2, and -72.2 Pa when it was 80 mm^2. In a previous study, [32] it was reported that the CSA of the site equivalent to the RA in OSA cases was 78.2 ± 50.1 mm^2 and 173 ± 97.6 mm^2 in non-OSA cases. Based on these previous findings, [32] as well as the results of the present study, we suggest that obstruction might occur due to a large negative pressure when the CSA of the RA is 100 mm^2 or less.

Furthermore, we evaluated the APD of the RA and its association with CFD values to determine the ventilation conditions reflected by the cephalometric images in our study. The relationship between the APD of the RA and Pmax was similar to that of the CSA of the RA and Pmax (Fig. 2A and 2B). This may be why the APD of the RA varied in previous study results. Our result showed a pressure of -36.7 Pa when the APD of the RA was 8 mm, and the pressure reduced to -50.1 Pa at an APD of 7 mm. A sudden decrease to -80 Pa was observed when the APD of the RA was 6 mm. Previous studies [24-26] have shown that the mean APD of the RA in cases of moderate to severe OSA is approximately 5 mm. We considered that our present study results corresponded to these previous studies. [24-26] The regression equation showed that a very large negative pressure of -100 Pa occurred at an APD of 5 mm, and changed markedly at 7 mm (Fig. 2B). Thus, CFD clearly showed the threshold value of an APD of the RA of 7 mm. CFD therefore clarified the complicated association between PA form and ventilation conditions, demonstrating the usefulness of the CFD study.

LIMITATIONS

This study had some limitations. Unlike some conventional methods that cannot separate PA, CFD can evaluate airflow in the PA alone, giving a more accurate evaluation of the effect of mandibular setback surgery. However, it was not a clinical study, and thus, it is necessary to confirm these results in a clinical study that measures parameters of the nasal and hypopharyngeal airway. Nevertheless, this study confirmed the clinical usefulness of evaluating the ventilation condition of the PA. Additional studies with larger sample sizes and long-term follow-up of PA changes are required to inform best practices for the prevention of OSA after mandibular setback surgery.

CLINICAL IMPLICATIONS

In this study, we elucidated the relationship between ventilation conditions in the PA in a 3D model with morphological parameters, using CFD. As a component of treatment planning for mandibular setback surgery, the determination of preoperative APD, using cephalometry and a 3D model, may facilitate the prediction of postoperative APD and PA ventilation condition with a predefined amount of mandibular retraction. As such, the amount of mandibular retraction may be reduced on an individual basis, depending on the risk of postoperative impact on the PA ventilation condition. Pmax demonstrated an inversely proportional relationship to the square of APD-RA. This relationship was in accordance with Bernoulli's law, and also nonlinear, as Pmax substantially increased even with a slight reduction of the APD-RA. In addition, pharyngeal airway pressure rapidly increases when the APD-RA is 7 mm or less. OSA symptoms are influenced by the total upper airway resistance, which comprises both nasal airway resistance and pharyngeal airway resistance (pharyngeal airway pressure/flow rate). Therefore, this rapid increase in pharyngeal airway resistance might become the primary or the secondary cause of OSA when the APD-RA is 7 mm or less. Furthermore, it must be considered that this threshold may not only apply to postoperative obstruction in skeletal Class III cases, but also preoperatively, and in cases of skeletal Class II.

References

1. Riley RW, Powell NB, Guilleminault C, Ware W. Obstructive sleep apnea syndrome following surgery for mandibular prognathism. *J Oral Maxillofac Surg.* 1987;45(5):450-452.

2. Degerliyurt K, Ueki K, Hashiba Y, et al. The effect of mandibular setback or two-jaws surgery on pharyngeal airway among different genders. *International journal of oral and maxillofacial surgery.* 2009;38(6):647-652.

3. Jeon JY, Kim TS, Kim SY, Park CJ, Hwang KG. Does the Pharyngeal Airway Recover After Sagittal Split Ramus Osteotomy for Mandibular Prognathism? *J Oral Maxillofac Surg.* 2016;74(1):162-169.

4. Tepecik T, Ertas U, Akgun M. Effects of bimaxillary orthognathic surgery on pharyngeal airway and respiratory function at sleep in patients with class III skeletal relationship. *J Craniomaxillofac Surg.* 2018;46(4):645-653.

5. Tselnik M, Pogrel MA. Assessment of the pharyngeal airway space after mandibular setback surgery. *J Oral Maxillofac Surg.* 2000;58(3):282-285; discussion 285-287.

6. Chen F, Terada K, Hanada K, Saito I. Predicting the pharyngeal airway space after mandibular setback surgery. *J Oral Maxillofac Surg.* 2005;63(10):1509-1514.

7. Hochban W, Schurmann R, Brandenburg U, Conradt R. Mandibular setback for surgical correction of mandibular hyperplasia--does it provoke sleep-related breathing disorders? *International journal of oral and maxillofacial surgery.* 1996;25(5):333-338.

8. Park SB, Kim YI, Son WS, Hwang DS, Cho BH. Cone-beam computed tomography evaluation of short- and long-term airway change and stability after orthognathic surgery in patients with Class III skeletal deformities: bimaxillary surgery and mandibular setback surgery. *International journal of oral and maxillofacial surgery.* 2012;41(1):87-93.

9. Kawamata A, Fujishita M, Ariji Y, Ariji E. Three-dimensional computed tomographic evaluation of morphologic airway changes after mandibular setback osteotomy for prognathism. *Oral Surg Oral Med Oral Pathol Oral Radiol Endod.* 2000;89(3):278-287.

10. Hasebe D, Kobayashi T, Hasegawa M, et al. Changes in oropharyngeal airway and respiratory function during sleep after orthognathic surgery in patients with mandibular prognathism. *International journal of oral and maxillofacial surgery.* 2011;40(6):584-592.

11. Uesugi T, Kobayashi T, Hasebe D, Tanaka R, Ike M, Saito C. Effects of orthognathic surgery on pharyngeal airway and respiratory function during sleep in patients with mandibular prognathism. *International journal of oral and maxillofacial surgery.* 2014;43(9):1082-1090.

12. Butterfield KJ, Marks PL, McLean L, Newton J. Linear and volumetric airway changes after maxillomandibular advancement for obstructive sleep apnea. *J Oral Maxillofac Surg.* 2015;73(6):1133-1142.

13. Iwasaki T, Saitoh I, Takemoto Y, et al. Evaluation of upper airway obstruction in Class II children with fluid-mechanical simulation. *Am J Orthod Dentofacial Orthop.* 2011;139(2):e135-145.

14. Zhao M, Barber T, Cistulli P, Sutherland K, Rosengarten G. Computational fluid dynamics for the assessment of upper airway response to oral appliance treatment in obstructive sleep apnea. *J Biomech.* 2013;46(1):142-150.

15. Wootton DM, Luo H, Persak SC, et al. Computational fluid dynamics endpoints to characterize obstructive sleep apnea syndrome in children. *J Appl Physiol (1985).* 2014;116(1):104-112.

16. Shah DH, Kim KB, McQuilling MW, Movahed R, Shah AH, Kim YI. Computational fluid dynamics for the assessment of upper airway changes in skeletal Class III patients treated with mandibular setback surgery. *Angle Orthod.* 2016;86(6):976-982.

17. Yajima Y, Oshima M, Iwai T, Kitajima H, Omura S, Tohnai I. Computational fluid dynamics study of the pharyngeal airway space before and after mandibular setback surgery in patients with mandibular prognathism. *International journal of oral and maxillofacial surgery.* 2017;46(7):839-844.

18. Suga H, Iwasaki T, Mishima K, Nakano H, Ueyama Y, Yamasaki Y. Evaluation of the effect of oral appliance treatment on upper-airway ventilation conditions in obstructive sleep apnea using computational fluid dynamics. *Cranio : the journal of craniomandibular practice.* 2019:1-9.

19. Muto T, Takeda S, Kanazawa M, Yamazaki A, Fujiwara Y, Mizoguchi I. The effect of head posture on the pharyngeal airway space (PAS). *International journal of oral and maxillofacial surgery.* 2002;31(6):579-583.

20. Iwasaki T, Takemoto Y, Inada E, et al. Three-dimensional cone-beam computed tomography analysis of enlargement of the pharyngeal airway by the Herbst appliance. *Am J Orthod Dentofacial Orthop.* 2014;146(6):776-785.

21. Souza Pinto GN, Iwaki Filho L, Previdelli I, et al. Three-dimensional alterations in pharyngeal airspace, soft palate, and hyoid bone of class II and class III patients submitted to bimaxillary orthognathic surgery: A retrospective study. *J Craniomaxillofac Surg.* 2019;47(6):883-894.

22. Gamiño B, Aguillón J. Numerical simulation of syngas combustion with a multi-spark ignition system in a diesel engine adapted to work at the Otto cycle. *Fuel.* 2010;89:581-591.

23. Downing JM, Ku DN. Effects of frictional losses and pulsatile flow on the collapse of stenotic arteries. *Journal of biomechanical engineering.* 1997;119(3):317-324.

24. Ogawa T, Enciso R, Shintaku WH, Clark GT. Evaluation of cross-section airway configuration of obstructive sleep apnea. *Oral Surg Oral Med Oral Pathol Oral Radiol Endod.* 2007;103(1):102-108.

25. Partinen M, Guilleminault C, Quera-Salva MA, Jamieson A. Obstructive sleep apnea and cephalometric roentgenograms. The role of anatomic upper airway abnormalities in the definition of abnormal breathing during sleep. *Chest.* 1988;93(6):1199-1205.

26. Sakakibara H, Tong M, Matsushita K, Hirata M, Konishi Y, Suetsugu S. Cephalometric abnormalities in non-obese and obese patients with obstructive sleep apnoea. *Eur Respir J.* 1999;13(2):403-410.

27. Abramson ZR, Susarla S, Tagoni JR, Kaban L. Three-dimensional computed tomographic analysis of airway anatomy. *J Oral Maxillofac Surg.* 2010;68(2):363-371.

28. Anegawa E, Tsuyama H, Kusukawa J. Lateral cephalometric analysis of the pharyngeal airway space affected by head posture. *International journal of oral and maxillofacial surgery.* 2008;37(9):805-809.

29. Mukaihara K, Hasegawa-Moriyama M, Iwasaki T, Yamasaki Y, Kanmura Y. Evaluation of the pharyngeal airway using computational fluid dynamics in

patients with acromegaly. *Laryngoscope investigative otolaryngology.* 2018;3(2):133-138.

30. Iwasaki T, Sato H, Suga H, et al. Herbst appliance effects on pharyngeal airway ventilation evaluated using computational fluid dynamics. *Angle Orthod.* 2017;87(3):397-403.

31. Iwasaki T, Sato H, Suga H, et al. Influence of pharyngeal airway respiration pressure on Class II mandibular retrusion in children: A computational fluid dynamics study of inspiration and expiration. *Orthod Craniofac Res.* 2017;20(2):95-101.

32. Peh WC, Ip MS, Chu FS, Chung KF. Computed tomographic cephalometric analysis of Chinese patients with obstructive sleep apnoea. *Australasian radiology.* 2000;44(4):417-423.

Figure Legends

Figure 1. Measurement of the maxillomandibular morphology pharyngeal airway. (A) Anteroposterior and vertical cephalometric landmark positions measured parallel and perpendicular to the FH plane: RL, Reference line (plane parallel to the FH plane passing through the sella); S, sella; A, A-point; B, B-point; H, hyoid bone; FH, Frankfurt horizontal. (B) Landmarks and planes for the axial airway section; RA pl, a plane parallel to the palatal plane passing through the narrowest point on the soft palate; CV_2 pl, a plane parallel to the palatal plane passing through the base of the second cervical vertebra; OA pl, a plane parallel to the palatal plane passing through the midpoint of gonion bilaterally; CV3pl, a plane parallel to the palatal plane passing through the base of the third cervical vertebra. (C) Cross-sectional areas of each pharyngeal airway. RA, retropalatal airway; CV_2A, CV_2 airway; OA, oropharyngeal airway; CV_3A, CV_3 airway; APD, anteroposterior depth; LAW, lateral width; CSA, cross-sectional area. (D) extraction of the pharyngeal airway data. (E) volume rendering and numeric simulation (light blue arrow, inlet air flow). (F) evaluation of pharyngeal airway ventilation condition using computational fluid dynamics. left; velocity, right; pressure.

Figure 2. Relationships between cross-sectional area (CSA) of the retropalatal airway (RA) and anteroposterior depth (APD) of the RA and maximum negative pressure (Pmax).

(A) Relationships between Pmax and CSA-RA. The non-linear regression equation describing the relationship between Pmax and CSA-RA represented a power function. The relationship between Pmax and CSA-RA is shown by the fitted curve, which is the inversely proportional curve between the preoperative and postoperative data. (B) Relationship between Pmax and APD-RA. One outlier case that had a shallow APD-RA (as the soft palate was thick, APD-RA was small) and low Pmax was excluded (red arrows; before and after surgery). The non-linear regression equation describing the relationship between Pmax and APD-RA represents a power function.

Figure 3. Different ventilation condition results for the same anteroposterior depth (APD) of the retropalatal airway (RA) after mandibular setback surgery. (A) small change case; left, before surgery; right, after surgery. (B) marked change case (left, before surgery; right, after surgery.

(A) Before surgery; APD-RA was fairly large (15.9 mm), and the maximum negative pressure (Pmax) was -7.0 Pa. After surgery; APD-RA was reduced to 11.5 mm. The Pmax was low (-15.2 Pa) after surgery. (B) Before surgery; APD-RA was relatively small (9.1 mm), and the pressure was -26.4 Pa. After surgery; APD-RA was reduced to 5.2 mm. After surgery, the Pmax was large (-101.7 Pa). This shows that the effect on ventilation condition varied according to the APD-RA size before surgery, even if the amount of change in APD-RA was similar.

Table 1. Statistical comparison of cephalometric measurements

	Before surgery		After surgery		Change		
	mean	SD	mean	SD	mean	SD	P
Ax (mm)	66.57	4.21	66.44	4.38	0.14	0.52	.268
Ay (mm)	32.68	3.55	32.40	3.43	0.28	0.59	.055
Bx (mm)	70.40	5.60	64.57	5.65	5.77	2.09	＜.001*
By (mm)	74.98	5.78	73.58	5.01	1.40	1.62	.001*
Hx (mm)	25.64	9.28	22.81	9.28	2.82	1.01	＜.001*
Hy (mm)	80.12	8.01	82.24	7.23	−2.11	2.76	.004*
SNA (degree)	80.74	2.86	80.79	2.92	−0.05	0.23	.281
SNB (degree)	82.18	2.69	79.66	2.55	2.53	1.65	＜.001*
ANB (degree)	−1.44	2.47	1.08	2.22	−2.58	1.61	＜.001*
ESS#	5.8	3.3	5.4	3.7	0.4	3.4	.639

Abbreviations: ESS, Epworth Sleepiness Scale; #, n = 18.

* P ＜ .01, Postoperative significant changes by paired t-test.

Table 2. Statistical comparison of pharyngeal airway morpholgy

		RA	CV_2A	OA	CV_3A	Maximum value	Intersite difference P	Intersite difference post hoc
APD								
Before surgery (mm)	mean	12.61	15.87	16.06	15.64		< .001†	12, 13, 14
	SD	2.53	2.57	2.78	2.82			
After surgery (mm)	mean	8.87	12.09	12.11	12.52		< .001†	12, 13, 14
	SD	2.38	2.22	3.16	3.13			
Change ratio (%)	mean	69.68	76.86	75.93	81.45		.156	
	SD	10.70	12.94	16.74	20.77			
P		< .001*	< .001*	< .001*	.002*			
LAW								
Before surgery (mm)	mean	24.20	26.70	30.98	31.68		.003†	13, 14
	SD	5.91	7.34	5.65	8.56			
After surgery (mm)	mean	20.59	22.66	26.02	28.22		.001†	14, 24
	SD	5.63	5.67	5.74	7.22			
Change ratio (%)	mean	86.42	87.23	84.79	94.58		.480	
	SD	18.11	16.44	15.01	29.91			
P		.001*	.001*	< .001*	0.099			
CSA								
Before surgery (mm^2)	mean	195.04	276.43	319.52	324.28		< .001†	12, 13, 14
	SD	53.53	74.57	96.13	97.84			
After surgery (mm^2)	mean	136.42	218.97	225.17	242.13		< .001†	12, 13, 14
	SD	53.07	63.00	45.91	77.13			
Change ratio (%)	mean	69.33	81.13	73.61	78.01		.283	
	SD	15.53	21.06	16.58	24.45			
P		< .001*	.001*	< .001*	.001*			
Velocity (m/s)								
Before surgery (m/s)	mean	3.13	2.35	2.55	2.32	3.23	< .001†	12, 13, 14
	SD	1.13	0.90	1.10	0.67	1.17		
After surgery (m/s)	mean	5.62	3.61	3.59	3.70	5.81	< .001†	12, 13, 14
	SD	2.54	1.18	1.09	2.01	2.51		
Change ratio (%)	mean	186.43	163.87	155.57	166.73	187.32	.001†	
	SD	62.13	56.60	55.72	88.16	61.32		
P		< .001*	.001*	.004*	.003*	< .001*		
Pressure (Pa)								
Before surgery (Pa)	mean	−9.30	−10.49	−12.97	−15.82	−16.05	< .001†	13, 14, 24, 34
	SD	7.39	8.25	10.92	11.99	12.07		
After surgery (Pa)	mean	−24.85	−29.71	−31.58	−39.13	−40.63	.008†	14, 24, 34
	SD	18.75	27.19	26.92	38.67	38.37		
Change ratio (%)	mean	407.55	366.10	360.74	317.63	328.65	.075	
	SD	241.19	215.32	244.57	227.98	212.70		
P		.001*	< .001*	.002*	.001*	.001*		

Abbreviations: RA, retropalatal airway; CV_2A, second cervical vertebral airway; OA, oropharyngeal airway; CV_3A, third cervical vertebral airway; APD, antero-posterior airway depth; LAW, lateral airway width, CSA; cross-sectional area; Change ratio, postsurgery value/presurgery value*100.

* P < .01, Postoperative significant changes by paired *t*-test. † P < .01, Intersite significant diferences by ANOVA with Bonferroni's correction: 12, RA vs. CV2A; 13, RA vs. OA; 14, RA vs. CV3A; 24, CV2A vs. CV3A;

Table 3 Correlation between pharyngeal airway morphology and ventilation condition

n = 38

	Maximum velocity		Maximum negative pressure	
	r_s	P	r_s	P
APD				
RA	−.643	< .001*	.628	< .001*
CV_2A	−.580	< .001*	.491	.002*
OA	−.507	.001*	.493	.002*
CV_3A	−.440	.006*	.466	.003*
CSA				
RA	−.847	< .001*	.848	< .001*
CV_2A	−.602	< .001*	.595	< .001*
OA	−.646	< .001*	.654	< .001*
CV_3A	−.529	.001*	.614	< .001*

Abbreviations: rs, Spearman's rank correlation coefficient; RA, retropalatal airway; CV_2A, second cervical vertebra airway; OA, oropharyngeal airway; CV_3A, third cervical vertebra airway; CSA; cross-sectional area; APD, antero-posterior airway depth.

* $P < .01$, Significant correlation coefficient.

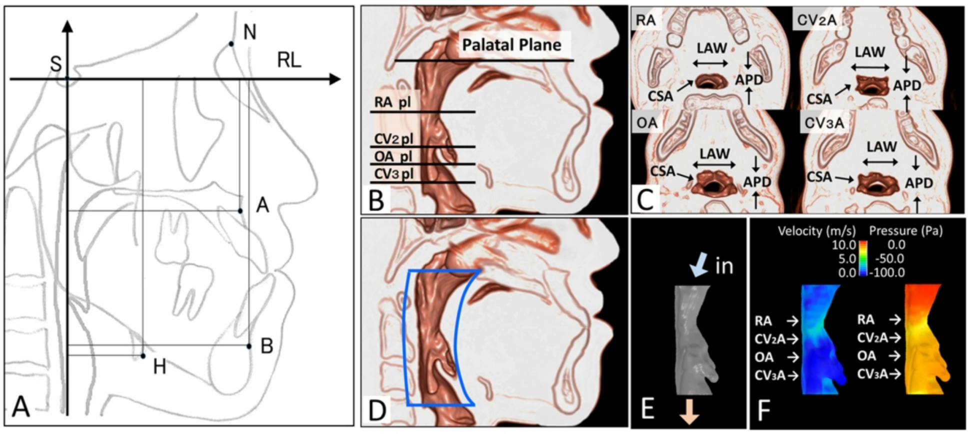

Figure 1 Measurement of the maxillomandibular morphology pharyngeal airway. (A) Anteroposterior and vertical cephalometric landmark positions measured parallel and perpendicular to the FH plane: RL, Reference line (plane parallel to the FH plane passing through the sella); S, sella; A, A-point; B, B-point; H, hyoid bone; FH, Frankfurt horizontal. (B) Landmarks and planes for the axial airway section; RA pl, a plane parallel to the palatal plane passing through the narrowest point on the soft palate; CV2 pl, a plane parallel to the palatal plane passing through the base of the second cervical vertebra; OA pl, a plane parallel to the palatal plane passing through the midpoint of gonion bilaterally; CV3pl, a plane parallel to the palatal plane passing through the base of the third cervical vertebra. (C) Cross-sectional areas of each pharyngeal airway. RA, retropalatal airway; CV2A, CV2 airway; OA, oropharyngeal airway; CV3A, CV3 airway; APD, anteroposterior depth; LAW, lateral width; CSA, cross-sectional area. (D) extraction of the pharyngeal airway data. (E) volume rendering and numeric simulation (light blue arrow, inlet air flow). (F) evaluation of pharyngeal airway ventilation condition using computational fluid dynamics. left; velocity, right; pressure.

508x381mm (96 x 96 DPI)

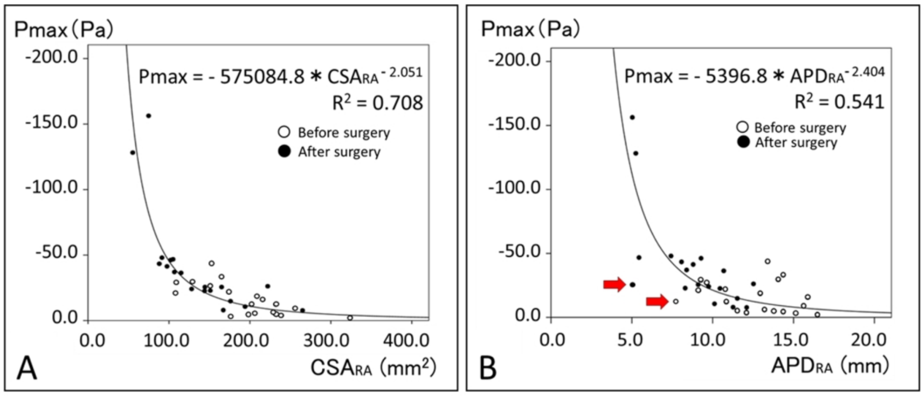

Figure 2 Relationships between cross-sectional area (CSA) of the retropalatal airway (RA) and anteroposterior depth (APD) of the RA and maximum negative pressure (Pmax).(A) Relationships between Pmax and CSA-RA. The non-linear regression equation describing the relationship between Pmax and CSA-RA represented a power function. The relationship between Pmax and CSA-RA is shown by the fitted curve, which is the inversely proportional curve between the preoperative and postoperative data. (B) Relationship between Pmax and APD-RA. One outlier case that had a shallow APD-RA (as the soft palate was thick, APD-RA was small) and low Pmax was excluded (red arrows; before and after surgery). The non-linear regression equation describing the relationship between Pmax and APD-RA represents a power function.

508x381mm (96 x 96 DPI)

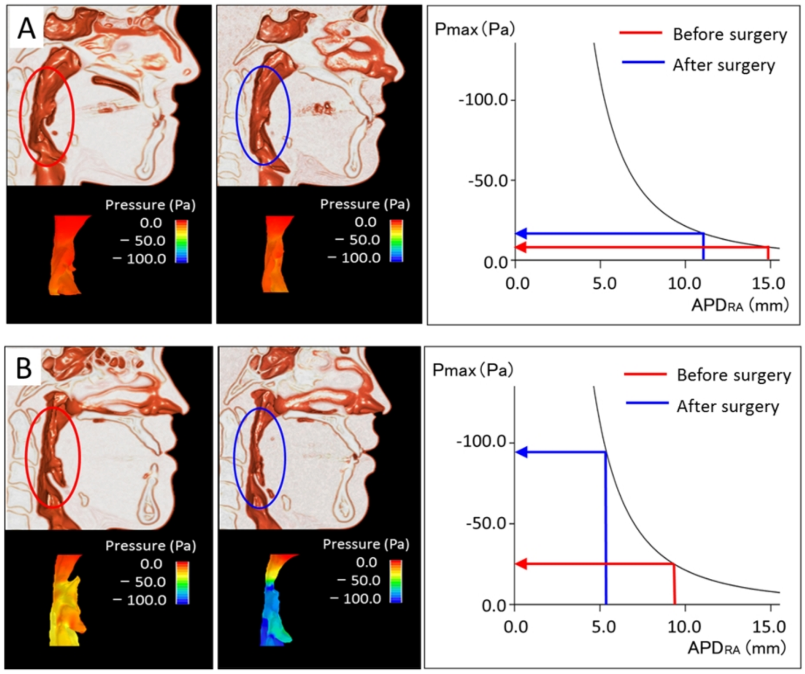

Figure 3 Different ventilation condition results for the same anteroposterior depth (APD) of the retropalatal airway (RA) after mandibular setback surgery. (A) small change case; left, before surgery; right, after surgery. (B) marked change case (left, before surgery; right, after surgery.(A) Before surgery; APD-RA was fairly large (15.9 mm), and the maximum negative pressure (Pmax) was -7.0 Pa. After surgery; APD-RA was reduced to 11.5 mm. The Pmax was low (-15.2 Pa) after surgery. (B) Before surgery; APD-RA was relatively small (9.1 mm), and the pressure was -26.4 Pa. After surgery; APD-RA was reduced to 5.2 mm. After surgery, the Pmax was large (-101.7 Pa). This shows that the effect on ventilation condition varied according to the APD-RA size before surgery, even if the amount of change in APD-RA was similar.

508x381mm (96 x 96 DPI)